



ELSEVIER

Available online at [www.sciencedirect.com](http://www.sciencedirect.com)

ScienceDirect

EPSL

Earth and Planetary Science Letters xx (2007) xxx–xxx

[www.elsevier.com/locate/epsl](http://www.elsevier.com/locate/epsl)

## Chicxulub impact predates K–T boundary: New evidence from Brazos, Texas

Gerta Keller<sup>a,\*</sup>, Thierry Adate<sup>b</sup>, Zsolt Berner<sup>c</sup>, Markus Harting<sup>d</sup>, Gerald Baum<sup>e</sup>,  
Michael Prauss<sup>f</sup>, Abdel Tantawy<sup>g</sup>, Doris Stueben<sup>c</sup>

<sup>a</sup> *Geosciences, Princeton University, Princeton NJ 08540, USA*

<sup>b</sup> *Geological Institute, University of Neuchatel, Neuchatel, CH-2007, Switzerland*

<sup>c</sup> *Institute for Mineralogy and Geochemistry, University of Karlsruhe, 76128 Karlsruhe, Germany*

<sup>d</sup> *Department of Earth Sciences, Utrecht University, Utrecht, The Netherlands*

<sup>e</sup> *Lewis Energy Group, 10101 Reunion Square, Suite 1000, San Antonio, Texas 78216, USA*

<sup>f</sup> *Free University Berlin, Institute for Geosciences, Section Paleontology, D-12249 Berlin, Germany*

<sup>g</sup> *Geology Department, South Valley University, Asswan, Egypt*

Received 20 July 2006; received in revised form 20 November 2006; accepted 22 December 2006

Editor: C.P. Jaupart

### Abstract

Multidisciplinary studies, including stratigraphy, sedimentology, mineralogy and geochemistry, of the new core Mullinax-1 and outcrops along the Brazos River and Cottonmouth Creek, Falls County, Texas, reveal the complex history of the Chicxulub impact, the event deposit and the K–T boundary event. The K–T boundary, as identified by the negative  $\delta^{13}\text{C}$  shift, first occurrence of Danian planktic foraminifera and palynomorphs occurs 80 cm above the event deposit in core Mullinax-1. The underlying 80 cm interval was deposited in a shallow low oxygen environment during the latest Maastrichtian, as indicated by high stress microfossil assemblages, small shells and burrows infilled with framboidal pyrite. The underlying event deposit, commonly interpreted as K–T impact tsunami, consists of a basal conglomerate with clasts containing Chicxulub impact spherules, repeated upward fining units of spherule-rich sands, followed by hummocky cross-bedded and laminated sands, which are burrowed by *Thalassinoides*, *Planolites* and *Ophiomorpha* and truncated by erosion. This suggests a series of temporally separated storm events with re-colonization of the ocean floor by invertebrates between storms, rather than a series of waning tsunami-generated waves. The lithified clasts with impact spherules at the base of the event deposit provide strong evidence that the Chicxulub impact ejecta layer predates the event deposit, but was eroded and re-deposited during the latest Maastrichtian sea level lowstand. The original Chicxulub ejecta layer was discovered in a 3 cm thick yellow clay layer interbedded in undisturbed late Maastrichtian clay- and mudstones 45 cm below the base of the event deposit and near the base of planktic foraminiferal zone CF1, which spans the last 300 kyr of the Maastrichtian. The yellow clay consists of cheto smectite derived from alteration of impact glass, as indicated by rare altered glass spherules with similar chemical compositions as reworked spherules from the event deposit and Chicxulub impact spherules from NE Mexico and Haiti. The Brazos sections thus provide strong evidence that the Chicxulub impact predates the K–T boundary by about 300 kyr, consistent with earlier observations in NE Mexico and the Chicxulub crater core Yaxcopoil-1.

© 2007 Published by Elsevier B.V.

**Keywords:** Chicxulub impact; Event deposit; K–T boundary; Brazos; Texas

\* Corresponding author.

E-mail address: [gkeller@princeton.edu](mailto:gkeller@princeton.edu) (G. Keller).

## 1. Introduction

The theory that a large meteorite impact on Earth caused the Cretaceous–Tertiary (K–T) mass extinction is widely believed as proven with the discoveries of the Chicxulub crater on Yucatan [1] and impact spherule ejecta at the base of a sandstone complex throughout Mexico and Central America in close stratigraphic proximity to the Cretaceous–Tertiary (K–T) boundary mass extinction and Ir anomaly [2–5]. Recently, this 25-year old theory has been challenged by investigations of the Chicxulub crater core Yaxcopoil-1 and localities throughout NE Mexico where the impact breccia and spherule ejecta, respectively, predate the K–T boundary and Ir anomaly by about 300,000 yr, suggesting a multiple impact scenario [4–7]. At issue are not only the pre-K–T age of the Chicxulub impact, which is based on the recent discovery in NE Mexico of the original impact spherule ejecta layer in marine marls 4–9 m below the sandstone complex, but also the nature and origin of this sandstone complex, which is commonly interpreted as a series of Chicxulub impact-generated tsunami waves [2,3], as well as the origin and cause for the K–T boundary mass extinction and Ir anomaly. Can these three stratigraphically separate events (in the most complete sequences) be reconciled as some complex scenario of Chicxulub impact-generated disturbance? Or, does it reveal a more complex scenario of two impacts, sea level and climate changes?

To test the challenging results from NE Mexico and the Chicxulub crater core Yaxcopoil-1, the National Science Foundation (NSF) supported new drilling by DOSECC (Drilling, Observation and Sampling of Earths Continental Crust) along the Brazos River, Falls County, Texas. This area was chosen for its ~1000 km distance from the impact crater, tectonically undisturbed sedimentary sequences, excellent preservation of microfossils, and the presence of a sandstone complex at the base of the Kincaid Formation, commonly known as ‘event deposit’, or sea level lowstand deposit. Even prior to the discovery of the Chicxulub impact crater, the event deposit was interpreted as a tsunami deposit generated by the yet to be found K–T boundary impact [8]. The subsequent discovery of the Chicxulub crater seemed to support such a scenario, but detailed sedimentological investigations and the presence of truncated burrowed horizons suggested deposition by multiple storms, rather than a single high-energy tsunami [9,10].

Drilling was successfully completed in March 2005 and together with fieldwork along the tributaries of the Brazos River recovered the most complete K–T sequences known in this area to date. Multidisciplinary investigations were conducted of the age, stratigraphy, mineralogy, geochemistry and depositional environment of the sequences containing Chicxulub ejecta in the new core Mullinax-1 and new Cottonmouth Creek outcrops (CMA-B, Fig. 1). This report focuses on: (1) the K–T boundary placement, (2) the age of the event deposit and



Fig. 1. Locations of K–T boundary sequences analyzed with Chicxulub ejecta in the US, Mexico, Guatemala, Belize and the Chicxulub crater [4–6,20]. Insert shows locations of the new and published Brazos River cores and outcrop sequences in Falls County, Texas. RB = River bed section [9]; KT1 and KT2 cores [13], KT3, CM1, CM4, Brazos-1, -2 and -3 [14,27], Mullinax-1 and CMA-B new core and outcrops (this study).

whether it can be considered coeval with the K–T boundary as claimed by many workers, (3) the origin of the event deposit, whether a direct result of Chicxulub impact generated tsunami or earthquake disturbance [2,3,8,11–13], or a consequence of storm deposits emplaced during the latest Maastrichtian sea level fall and following early transgression [9,10,14], and (4) the age of the Chicxulub impact as determined from the impact ejecta layers in the Brazos sequences.

### 1.1. Location of Brazos sections

Core Mullinax-1 (Mull-1) is located on a meadow about 370 m downstream from the Highway 413 Bridge over the Brazos River, Falls County, Texas (GPS Location 31° 07'53. 00"N, 96° 49'30. 14"W; Fig. 1). This is the same location where cores KT1 and KT2 were rotary drilled in the middle 1980's, but encountered drilling disturbance in KT1 [10, Hansen, pers. commun. 1988, 2005] and which Schulte et al. [13] studied. The new core Mull-1 provides continuous (100%) and undisturbed core recovery from the early Danian through the late Maastrichtian and permits evaluation of the event deposit and the K–T boundary. The Cottonmouth Creek is a small tributary of the Brazos River about 1.8 km down river from the Highway 413 Bridge and 1.2 km from the Mull-1 core (Fig. 1). At this locality the CMA-B section was collected in two segments 20 m apart. The outcrop exposure at CMA spans from 1.2 m below the event deposit to 25 cm above, whereas at CMB the event deposit and overlying 1–2 m of sediments are exposed.

## 2. Methods

In the field, the outcrops were carefully studied, measured, described, photographed and sampled at an average of 5 cm intervals with 1–2 cm spacing through critical intervals. The cores were split, photographed and described for the record and the working half core sampled at 5–10 cm interval with 1–2 cm sample spacing in critical intervals. Samples were distributed among the various team members for study. For biostratigraphic analyses (planktic foraminifera, nannofossils and palynomorphs), samples were processed by standard techniques [15,16]. Bulk and clay mineral analyses were based on XRD analyses (SCINTAG XRD 2000 Diffractometer). Sample processing followed published procedures [17,18]. The origin and amount of organic matter were determined by Rock-Eval pyrolysis using a Rock-Eval 6 [18]. Granulometry was achieved using a Laser Particles Sizer (LOT GmbH).

Stable isotope analysis was performed on fine fraction carbonate (38–63  $\mu\text{m}$ ) and the benthic foraminifer *Lenticulina* sp. using a fully automated carbonate preparation system (MultiCarb) connected on-line to an isotope ratio mass spectrometer (Optima, Micromas Ltd., UK). Isotope ratio values are reported relative to NBS-19 with  $\delta^{13}\text{C}=1.95\text{‰}$  (V-PDB). Precision, assessed on the basis of repeated measurements of the carbonate standard, was generally better than 0.06‰ for each analytical batch. Spherule geochemistry was analyzed by raster electron microscopy (REM), back-scatter electron imaging (BSE), wavelength-dispersive (WDS) and energy-dispersive (EDS) electron microprobe of polished and carbon coated thin sections. Major element concentrations are reported as weight percent (wt%) normalized to 100% of relative atomic proportions using the Cameca SX50 Geostandard software.

## 3. Sedimentology, mineralogy and stratigraphy

In the Brazos River area, late Maastrichtian sediments are commonly assigned to the Corsicana/Kemp Formation with earliest Tertiary sediments (Danian zones P0 to P1b) assigned to the Littig Member of the Kincaid Formation. In practice, the Corsicana/Kemp Formation is assigned to the late Maastrichtian below the event deposit and the Kincaid Formation to sediments above it. Yancey [9] proposed subdivision of the event deposit into distinct lithological units, which are followed here.

### 3.1. Cottonmouth creek CMA-B section

#### 3.1.1. Latest Maastrichtian

Sediments below the event deposit in the CMA-B section consist of undisturbed, dark grey, thinly bedded claystone with macrofossils and burrows (Fig. 2, units A<sub>1</sub>, A<sub>3</sub>). TOC is relatively high (0.6–1%), phyllosilicates average 50–60%, smectites 60–70% (relative to phyllosilicates, except for one peak of 100%), and calcite is a steady low ~10% (Fig. 3A).  $\delta^{13}\text{C}$  values are relatively constant for fine fraction (–0.5 to 0‰) and *Lenticulina* sp. (–1 and 0‰). At 40 cm below the event deposit there is a prominent 3 cm thick yellow clay layer that can be traced laterally over 20–30 m depending on outcrop exposure. This yellow clay consists of 100% cheto Mg-smectite derived from altered Chicxulub impact glass with the same composition as in the spherule-rich coarse sandstone (SCS) of the event deposit (Section 4.2). Cheto smectite is an almost pure high Mg-smectite that



forms up to 100% of the clay fraction and is interpreted to have derived from weathering of impact glass (e.g. melt rock and vapor condensates [19,20]. Cheto smectite clay is characterized by a high percentage of expendable layers (>95%), excellent crystallinity, very high intensity of the 001 reflection and a webby morphology. It has been widely observed in altered impact glass spherule deposits in Guatemala, Belize and Central Mexico [4,6,19,20]. Microfossils indicate a Latest Maastrichtian age for the interval below the event deposit based on the *Micula prinsii* nannofossil zone and planktic foraminiferal zone CF1 with the first appearance of the index species *Plummerita hantkeninoides* at 20 cm below the yellow clay (Fig. 2).

### 3.1.2. Event deposit

The most distinct feature of the CMA-B outcrops, and all Brazos sections in general, is the sandstone complex known as ‘event deposit’ that overlies a scoured channel surface. Throughout the Brazos area this sandstone complex is highly variable laterally and in thickness [9,10] due to the outcrop position within the channel (e.g., center or edge) and whole or partial removal of beds by scour induced by successive high-energy events. At the CMA-B outcrop the thickness of the event deposit varies from 10 cm to 65 cm over a distance of only 20–30 m and overlies the scoured base of a channel (Fig. 2). At its maximum development there is a 10 cm thick basal conglomerate bed (BCB) of locally derived clasts (Fig. 4A, B) from the underlying

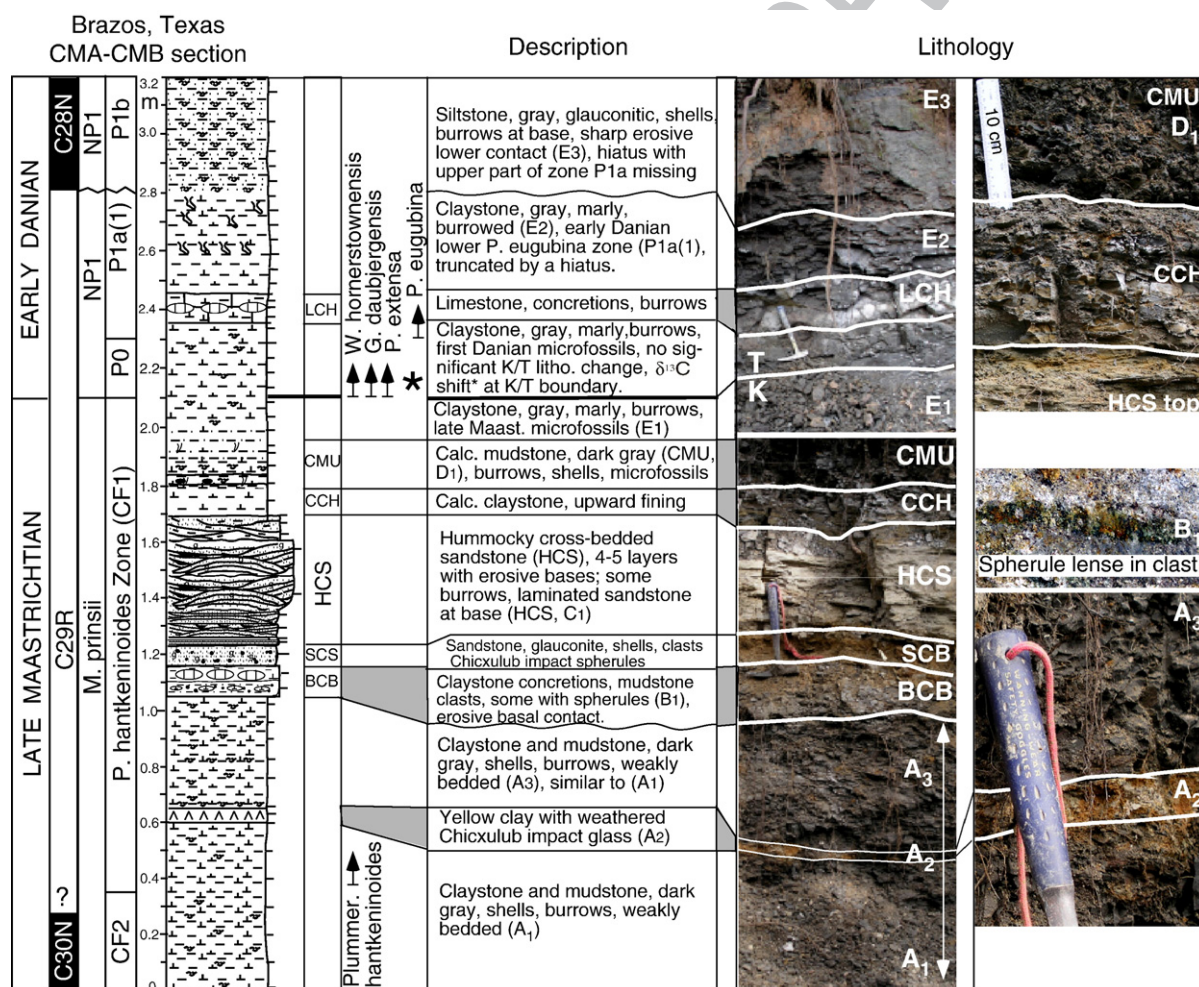


Fig. 2. Lithology and description of outcrops CMA-B across the event deposit and K–T boundary. Repeated truncated and frequently burrowed sandstone units of the event deposit indicate storm deposition. The K–T boundary is characterized by the negative  $\delta^{13}C$  shift and faunal and floral turnovers 30 cm above the event deposit. A 3 cm thick yellow clay marks the original Chicxulub ejecta layer now altered to cheto smectite about 40 cm below the event deposit.

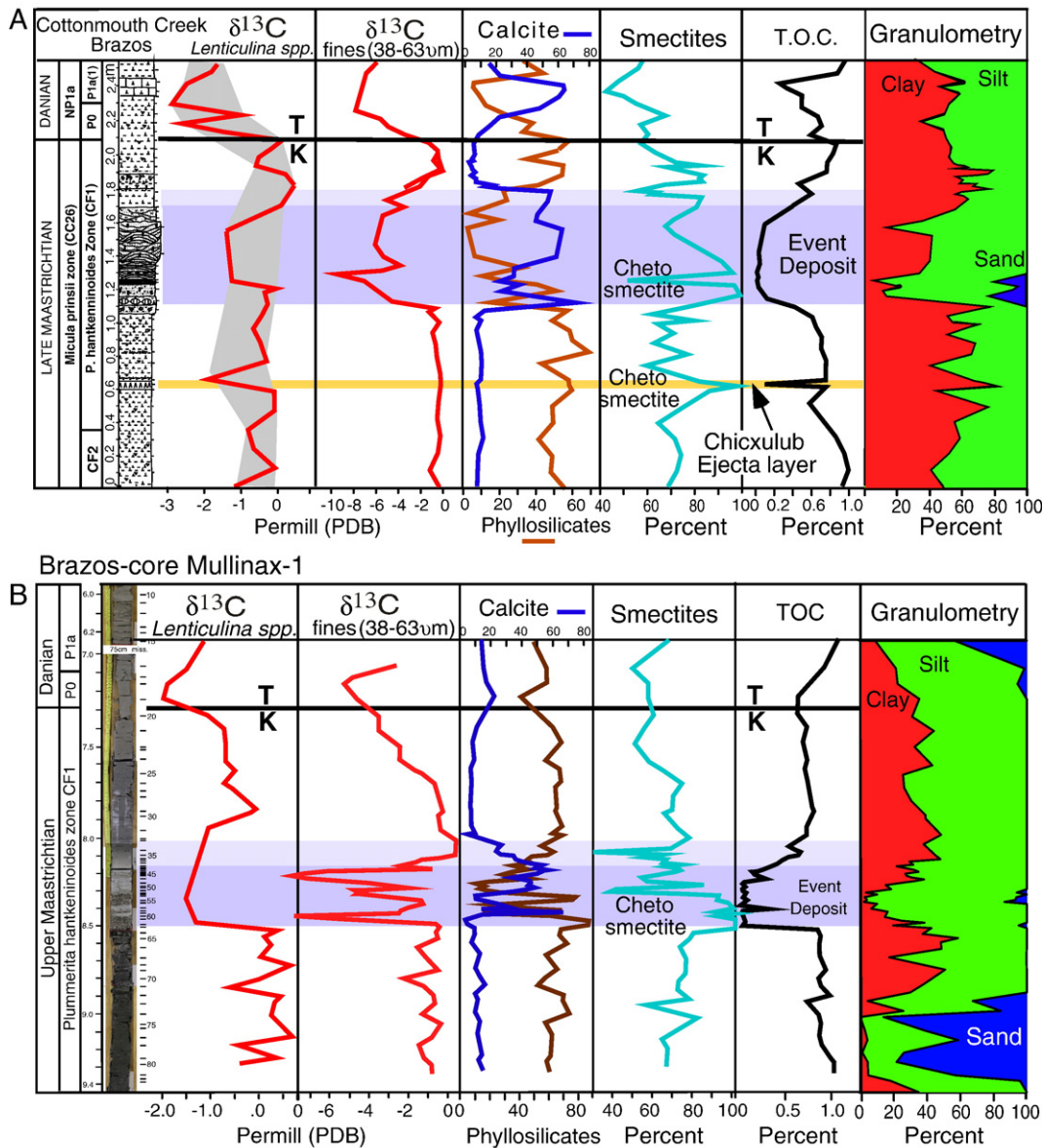


Fig. 3. A, B. Mineralogic, geochemical and granulometric data above and below the event deposits in the CMA-B section (A) and core Mullinax-1 (B) reveal normal late Maastrichtian marine sedimentation patterns. The K–T boundary is characterized by the negative  $\delta^{13}\text{C}$  shift and faunal and floral turnovers. Chicxulub impact glass spherules in the event deposit and the yellow clay 40 cm below (A) are marked by 100% Cheto smectite. The absence of the cheto smectite clay below the event deposit in Mullinax-1 (B) appears to be due to erosion and sand deposition.

222 mudstone [9]. The lithified mudstone clasts derived  
 223 from hemipelagic facies, as indicated by late Maas-  
 224 trichtian planktic foraminifera. They also reveal a  
 225 complex depositional history of the Chicxulub impact  
 226 spherules.

227 For example, some clasts contain lenses of impact  
 228 spherules (Fig. 2, unit B<sub>1</sub>). Other clasts contain  
 229 morphologically well-preserved spherules (Fig. 4C, D),  
 230 which were incorporated into the sediments prior to

lithification, erosion, transport and re-deposition in unit  
 BCB. In some clasts there are fractures, or cracks,  
 infilled with spherules and the fractures rimmed by  
 several generations of sparry calcite, then truncated and  
 followed by normal sedimentation (Fig. 4E, F). This  
 suggests complex diagenetic processes and possible  
 emergence prior to erosion and transport. These clasts  
 with impact spherules provide very strong evidence of  
 the existence of an older spherule–ejecta layer, which



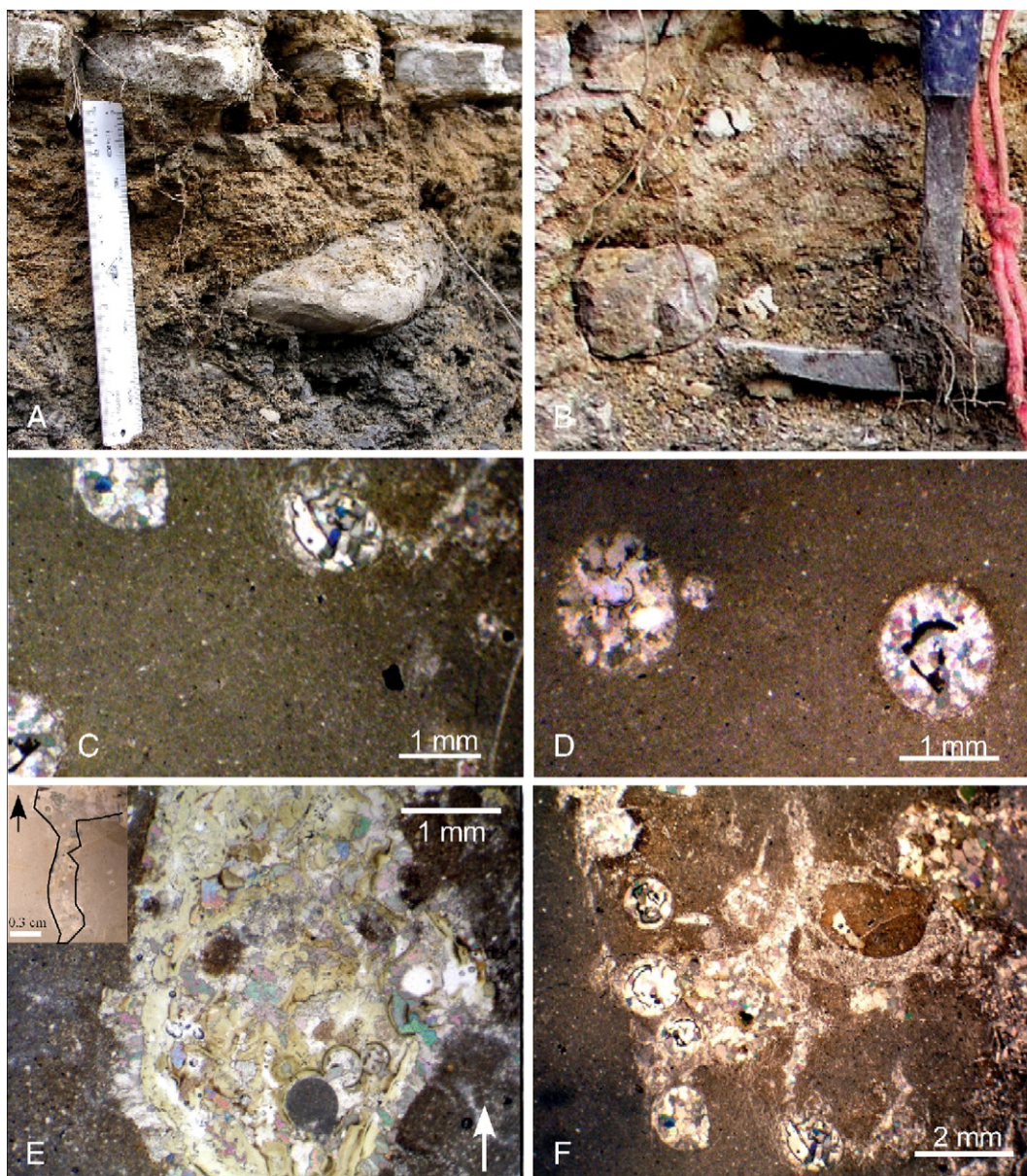


Fig. 4. A, B: Clasts from the basal conglomerate (BCB) of the event deposit contain Chicxulub impact spherules. C, D: spherules in mudstone clasts. E, F: spherules within cracks of mudstone clasts. E: cracks rimmed by sparry calcite. Insert shows morphology of crack and total length of ~2 cm. F: clast with cracks infilled with spherules and sparry calcite, then truncated by erosion and followed by normal sedimentation. These clasts reveal a history of Chicxulub ejecta fallout and lithification well prior to exposure to erosion, transport and redeposition at the base of the event deposit.

240 was lithified and subsequently eroded, transported and  
241 redeposited at the base of the event deposit.

242 The overlying spherule-rich coarse sandstone (SCS,  
243 unit SCB [9]) consists of green to brown sandstone with  
244 phosphatic clasts, glauconite, spherules and small  
245 (<1 cm) shale and mudstone clasts. Fine fraction  $\delta^{13}\text{C}$   
246 values are highly negative (up to  $-10\%$ ) and possibly  
247 reflect diagenetic cement. TOC is very low (<0.1%).

Above and below the event deposit, smectites average  
70%, but abruptly reach 100% (relative to the total  
amount of phyllosilicates) in the spherule-rich coarse  
sandstones (SCS, Fig. 3A). As in the yellow clay layer  
below, the smectite consists of pure Mg-smectite (cheto  
smectite), derived from altered Chicxulub impact glass.

The hummocky cross-bedded unit (HCS, Fig. 2)  
above the SCS is 40 cm thick and shows 3–4 laminated



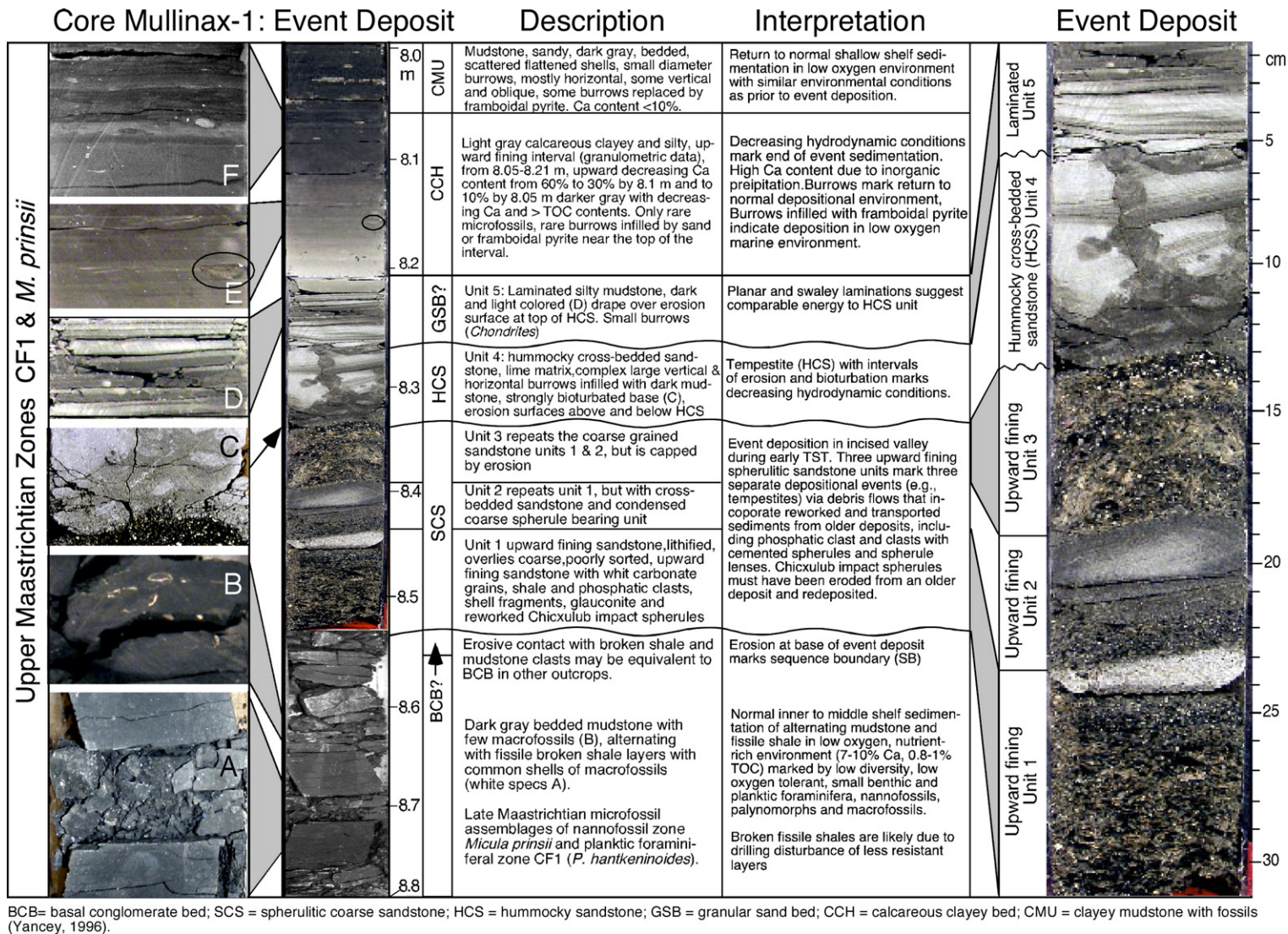


Fig. 5. Lithology, description and interpretation of the event deposit in core Mullinax-1. Note the three upward fining glauconitic spherule-rich coarse sandstone units topped by fine sandstone layers (unit SCS) and the truncated burrows in unit HCS. These are diagnostic features of multiple storm deposits.

sandstones with burrows, shells (*Thalassinoides* sp., *Planolites* sp.) and erosive bases. This indicates repeated significant energy depositional events separated by erosion and burrowing. In the nearby Brazos River bed exposures, Gale [10] documented up to five upward fining events with HCS and ripples, burrowed by *Ophiomorpha* and other organisms. Above unit HCS in the CMA-B sections there is a 10 cm thick calcareous claystone (Fig. 2, unit CCH) with upward fining grain size (granulometric data), increasing TOC, high calcite (50%), but very rare calcareous microfossils (Fig. 3A). The high carbonate and rare microfossils suggests fine mud settling. The CCH interval effectively ends event deposition and signals the return to normal sedimentation in the Brazos area.

### 3.1.3. Event deposit to K–T boundary

Above unit CCH, the clayey mudstone unit (CMU) is strongly burrowed with truncated burrows indicating erosion and a condensed sequence (Fig. 2). Some burrows are infilled with framboidal pyrite. Above the burrowed horizon, is a dark grey marly claystone with burrows, shells and late Maastrichtian low oxygen tolerant benthic and planktic microfossils. Shallow shelf sedimentation, similar to below the event deposit, returns in this interval with 9–10% calcite, relatively high TOC (0.7–0.8%), high phyllosilicate and lower smectites (Fig. 3A).  $\delta^{13}\text{C}$  values of bulk rock and *Lenticulina* sp. also return to pre-event deposit values. Microfossil assemblages indicate the latest Maastrichtian planktic foraminiferal zone CF1, nannofossil zone *M. prinsii*, and late Maastrichtian palynomorphs.

The K–T boundary as defined worldwide by the first appearance of Danian species (*W. hornerstownensis*, *G. daubjergensis*, *P. extensa*), nannofossils *M. prinsii*/NP1 zone boundary and the negative  $\delta^{13}\text{C}$  shift is 40 cm above unit HCS, or 30 cm above the upward fining unit CCH (Fig. 2). There is no significant lithological change across the K–T boundary. Sediments consist of calcareous mudstone with shells, few burrows and common Late Maastrichtian planktic foraminifera, nannofossils and palynomorphs.

25 cm above the K–T boundary is a 10 cm thick calcareous nodular horizon, termed the lower concretion horizon (LCH) by Yancey [9] to distinguish it from two upper concretions horizons of the Pisgah member of the Kincaid Formation. The LCH is just above the base of zone P1a. The overlying 30 cm of claystone are strongly burrowed. A sharp erosive contact separates this interval from the overlying grey, glauconitic siltstone with common shells and burrows at the base. Zone P1a abruptly terminates at this hiatus with the upper part of

the zone missing. The overlying siltstone is in Zone P1b, as indicated by the abrupt change in planktic foraminifera from by *Guembelitra*-dominated to *G. daubjergensis*-dominated assemblages and the abrupt appearances of *Parasubbotina pseudobulloides*, *P. varianta*, *Subbotina triloculinoides*, *Praemurica taurica*, *P. compressa* and *Eoglobigerina edita*.

### 3.2. Core mullinax-1 (Mull-1)

Mull-1 drilled through soil, unconsolidated sand and an aquifer down to 5.4 m. In the underlying sediments, the event deposit was encountered between 8.21–8.53 m. For this study the interval from 7 m to 8.8 m was analyzed at 1 to 5 cm intervals spanning the early Danian, K–T boundary, event deposit and underlying sediments.

#### 3.2.1. Latest Maastrichtian

In core Mull-1, the interval directly below the event deposit examined for this report (8.8–8.53 m) consists of dark grey horizontally bedded mudstone with relatively few invertebrate shells (Fig. 5-B) alternating with more fissile broken shale layers with more common shells (Fig. 5-A). There is no evidence of reworking (e.g., clasts, abraded and discolored foraminifera) in these sediments, which contain Late Maastrichtian microfossil assemblages (planktic foraminifera, nannofossils and palynomorphs) of CF1 and *Micula prinsii* zones with similar relative species abundances in mudstone and fissile shales. Mineralogically, the interval has low calcite (~10%), high phyllosilicates (60–80%) mainly composed of smectite (60–70%) and relatively high total organic content (TOC, ~0.8–1.0%, Fig. 3B). Granulometric data reflect the clay/silt variations between 8.53–8.9 m overlying a sand layer. Carbon isotopes show relatively stable Late Maastrichtian values in fine fraction (–0.5 to –1.5‰) and the benthic foraminifer *Lenticulina* (–0.5 to +0.5‰). These data suggest that the clay/silt alternations represent normal Late Maastrichtian shallow shelf sedimentation, whereas the underlying sand layer may be related to the sea level regression that culminated in the erosional unconformity at the base of the event deposit. The yellow clay (cheto smectite) layer from the CMA-B section, which stratigraphically correlates with this sand layer, is missing.

#### 3.2.2. Event deposit

In the Mull-1 core, erosion marks the base of the event deposit with an indistinct broken mudstone (3–5 cm) possibly representing the basal conglomerate bed



(BCB, Fig. 5). Above this layer, the event deposit can be subdivided into five distinct units. Units 1 to 3 are 8.5 cm, 4.5 cm and 5 cm thick, respectively, and correspond to the spherule-rich coarse sandstone unit (SCS). In each of these three units, the lower part consists of grey, green and brown coarse, poorly sorted, upward fining sandstones with abundant shell fragments, glauconite, small mudstone and phosphatic clasts, and (Chicxulub) impact spherules (Fig. 2). The upper part in units 1 and 2 grade into thin layers (1.5 cm to 2 cm) of light grey, cemented, rippled or cross-bedded

sandstone beds, though this part is eroded in unit 3. These units are diagnostic of storms with high-energy debris flows followed by upward waning energy depositing the rippled sandstone.

Geochemical and mineralogical analyses of the SCS bed show very similar results to the CMA-B section with very low TOC (<0.1%), a drop to <10% phyllosilicates (except for unit 3) and variable calcite (due to abundance of shells, Fig. 3B). Fine fraction  $\delta^{13}\text{C}$  values are highly negative overall (up to  $-7\text{‰}$ , similar to the CMA-B section). Smectites, which average 70%

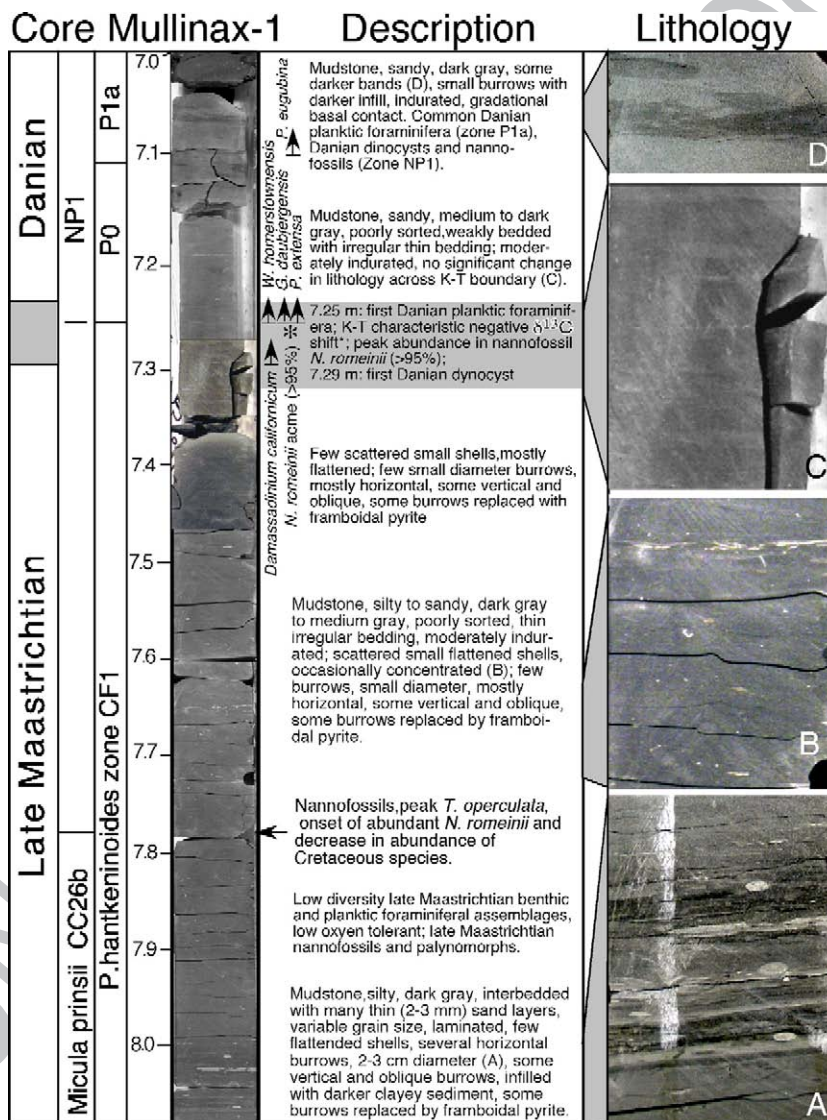


Fig. 6. Lithology and description of core Mullinax-1 between the event deposit and early Danian. Normal marine deposition is indicated by the bedded mudstones, shells, and burrows, some are infilled with framboidal pyrite indicating a low oxygen environment. Microfossil assemblages and  $\delta^{13}\text{C}$  data indicate a Late Maastrichtian age with the K–T boundary at 80 cm above the event deposit, as also supported by mineralogical data (Fig. 3B).

in late Maastrichtian sediments, abruptly reach 100% in the spherule-rich sandstone (SCS, Fig. 3B) where they consist of cheto smectite derived from altered Chicxulub impact glass.

An erosional surface separates the coarse spherule-rich sandstone (SCS) from the overlying hummocky cross-bedded sandstone (HCS) of unit 4. The base and top of the 6 cm thick HCS unit is strongly burrowed (Fig. 5). A large, complex burrow, infilled by darker mudstone, cuts vertically through this unit and is truncated by erosion at the top. The darker infilling sediment indicates that the burrows originated from a horizon that was subsequently eroded. Burrows within this unit were previously observed as *Ophiomorpha nodosa* [2], *Thalassinoides* sp. and *Planolites* sp. [10]. Granulometric data of the HCS interval show upward fining sandstone and a concurrent increase is observed in phyllosilicates (Fig. 3B). Calcite is high (40–60%) and in the absence of shells likely reflects diagenetic cementation.

Above the disconformity at the top of HCS is the 5 cm thick unit 5 (8.21–8.26 m), which consists of calcareous light and darker grey fine sandstone or silty mudstone with swaley and horizontal laminations that drape the underlying erosion surface and indicate comparable energy to the HCS unit 4 (Fig. 5-D). Small burrows are present. This unit may correspond to the granular sand bed (GSB) of Yancey [9]. From nearby Brazos River bed outcrops, Gale [10] identified *Thalassinoides* sp. and *Planolites* sp. burrows in this unit. Late Maastrichtian palynomorphs and planktic foraminiferal zone CF1 and nannofossil *M. prinsii* zone assemblages are common in units 4 and 5 (HCS and GSB) as well as above the event deposit.

The calcareous clayey horizon (CCH) marks the last stage of the event deposit. In Mull-1, this interval is represented by the 16 cm thick (8.05–8.21 m) calcareous silty claystone with upward fining grain size (granulometric data, Fig. 3B) and grading from light grey at the bottom to darker grey at the top (Fig. 5-E and F). Calcite decreases from a maximum of 60% at the base to 10% at the top, which is the norm for Brazos sediments in general (Fig. 3B). Decreasing calcite is accompanied by increasing phyllosilicates, darker color and higher TOC, returning to pre-event values at the top of CCH. No impact ejecta material is present either as spherules or altered glass (cheto smectite). Thin silt layers and lenses and some large (~3 cm) and small diameter burrows infilled with sand or framboidal pyrite are observed in the upper part (Fig. 5-F). Microfossils are rare in this interval. The decreasing grain size and increasing TOC suggest low energy currents, settling

from the water column and a gradual return to normal shelf sedimentation. The unusually high calcite content for Brazos in the near absence of calcareous microfossils is likely due to inorganic precipitation and settling of fine mud particles. Pyrite infilled burrows near the top indicate low oxygen bottom water conditions [21].

### 3.2.3. Event deposit to K–T boundary

Normal shallow shelf sedimentation resumed after the event deposit as indicated by the dark grey laminated mudstones with discrete burrows, which mark typical dysaerobic biofacies [21] characteristic of ichnofabric index 2 [22] (Fig. 6-A). Burrows are infilled with sand, mudstone or framboidal pyrite. Between 8.0 and 7.25 m, dark to medium grey silty to sandy, moderately indurated mudstones with irregular bedding prevail. Granulometric data reflect the same clay/silt ratios as below the event deposit (Fig. 3B). Scattered and usually flattened macrofossils are sometimes concentrated in thin layers (Fig. 6-B). Burrows are few and frequently replaced by framboidal pyrite, suggesting a low oxygen environment [21]. Late Maastrichtian planktic foraminifera and palynomorph assemblages prevail throughout this interval. All mineralogical and geochemical indicators, including phyllosilicates, carbonate, TOC and  $\delta^{13}\text{C}$ , return to pre-event late Maastrichtian values between the event deposit and K–T boundary, though bulk rock  $\delta^{13}\text{C}$  values and smectites gradually decrease at 7.65 m (Fig. 3B).

The K–T boundary characteristic  $\delta^{13}\text{C}$  negative excursion, which marks the K–T boundary worldwide, coincides with the extinction of most Cretaceous planktic foraminifera between 7.25–7.30 m. The first appearances of Danian planktic foraminifera (*Woodringina hornerstownensis*, *Parvularugoglobigerina extensa*, *Globigerina daubjergensis*), which are usually found within a few cm of the iridium anomaly and  $\delta^{13}\text{C}$  shift worldwide, occur at 7.25 m. The first Danian palynomorph *Damasadinium californicum*, a global K–T marker, first appears at 7.29 m (Fig. 6). These K–T markers thus identify the boundary about 80 cm above the event deposit (CCH) in core Mull-1. However, calcareous nannofossils show the biotic stress usually associated with the K–T boundary event already earlier beginning at 7.78 m. At this interval, Cretaceous species decrease *Thoracosphaera operculata* peaks at 20%, followed by a major increase in *Neobiscutum romeinii* (95%) up to the K–T boundary defined by the  $\delta^{13}\text{C}$  shift, foraminifera and palynomorphs. This phenomenon is still being studied (Thibault and Gardin, written communication 2006). No significant lithological change occurs in this interval, or the K–T boundary, similar to the CMA-B section (Fig. 6-C). The basal



Danian zone P0 spans 15 cm to the first appearance of *Parvularugoglobigerina eugubina* at 7.1 m. Above this interval, grey silty mudstones contain darker grey claystone layers (Fig. 6-D).

#### 4. Geochemistry of chicxulub impact ejecta

##### 4.1. Impact glass spherules

Altered glass spherule samples were analyzed in the event deposit from clasts of the basal conglomerate (BCB, Brazos spherules #1) and the spherule-rich coarse sandstone (SCS, Brazos spherules #2). In addition, smectite weathered spherules from the yellow clay below the event deposit at the CMA-B section were analyzed. Results show very similar compositions for the yellow clay and Brazos spherules #1 samples with 48–50% SiO<sub>2</sub>, 15–18% FeO, 10–12% Al<sub>2</sub>O<sub>3</sub>, 3–4% MgO and 1.3–1.7% CaO (Table 1). In contrast, Brazos spherules #2 exhibit lower FeO (2–3%), higher CaO (3–4%) and lower total oxides (81%), which reflects more

intense weathering through hydration or oxidation. These differences are also apparent in the ternary diagrams (CaO–(FeO+MgO)–(K<sub>2</sub>O+Na<sub>2</sub>O), which show the smectite weathered spherules from the yellow clay layer with the same chemical trend as Brazos spherules #1 (Fig. 7A, C), but the Brazos spherules #2 sample with more variable CaO (Fig. 7B). The yellow clay layer and Brazos spherules #1 data closely correlate with Fe-rich spherules from NE Mexico and Haiti (Fig. 7D) [23–25].

##### 4.2. Original Chicxulub impact–ejecta layer

We discovered what appears to be the undisturbed original impact spherule ejecta layer now altered to a 3 cm thick yellow clay 40 cm below the event deposit in outcrop CMA-B (Fig. 2). In the yellow clay, as well as the clay in the spherule-rich coarse sandstone (unit SCS) of outcrops CMA-B and Mull-1, smectites consist of 100% Mg-smectite (Fig. 3A and B). Mg-smectite is derived from weathering of glass (001 reflection, low

Table 1

Geochemical analyses of Chicxulub impact spherules from the event deposit and yellow clay (cheto smectite) at Brazos, Texas, compared spherule compositions from Beloc, Haiti, and La Sierrita, NE Mexico [13,24]

Location/samples	Impact glass type		MnO	FeO	NiO	SiO <sub>2</sub>	MgO	K <sub>2</sub> O	CaO	TiO <sub>2</sub>	Cr <sub>2</sub> O <sub>3</sub>	Na <sub>2</sub> O	Al <sub>2</sub> O <sub>3</sub>	Total
<i>Texas, Brazos</i>														
Yellow clay layer	Smectite spherules	Avg.	0.02	18.07	0.02	47.67	3.52	4.51	1.34	0.08	0.02	0.08	10.28	85.61
CMA-B section	<i>n</i> =48	SD	0.01	3.68	0.01	2.07	0.25	1.05	0.67	0.04	0.02	0.03	1.79	3.48
Brazos spher. #1	Smectite spherules	Avg.	0.02	15.55	0.02	50.13	4.18	4.89	1.7	0.11	0.02	0.09	12.73	89.44
Event deposit (BCB)	<i>n</i> =250	SD	0.01	2.47	0.02	2.47	0.73	1.21	0.46	0.08	0.02	0.04	1.85	4.72
Brazos spher. #2	Smectite spherules	Avg.	0.02	2.4	0.02	51.1	3.23	0.45	3.35	0.38	0.01	0.11	19.63	80.7
Event deposit (SCS)	<i>n</i> =250	SD	0.01	0.91	0.01	5.05	0.53	0.21	1.6	0.12	0.01	0.04	2.63	6.75
<i>Haiti</i>														
Beloc	Black glass spherules	Avg.		5.31		66.85	2.75	1.53	5.38	0.55		1.96	14.94	99.52
Stueben et al., 2002		SD		0.36		1.28	0.2	0.11	0.54	0.05		0.36	0.29	
Beloc	Yellow glass spherules	Avg.		5.37		60.47	3.16	1.4	11.45	0.65		2.78	14.21	99.63
Stueben et al., 2002		SD		0.6		4.49	0.55	0.42	5.29	0.06		0.3	0.82	
Beloc	Smectite spherules	Avg.		5.07		61.98	3.92	1.13	1.06	0.81		0.05	9.82	83.44
Stueben et al., 2002		SD		1.81		4.41	1.42	0.49	0.29	0.13		0.02	3.25	
Beloc	Smectite spherules	Avg.		4.81		65.26	4.64	1.1	0.88	0.34		0.06	11.12	88.23
Stueben et al., 2002		SD		0.41		3.21	0.4	0.43	0.16	0.13		0.02	0.83	
<i>NE Mexico</i>														
La Sierrita	Fe-rich spherules	Avg.		23.69		27.44	11.8	0.31	0.55	0.25		0.05	20.99	85.09
Schulte et al., 2006		SD		1.87		1.62	0.85	0.34	0.2	0.52		0.03	1.16	
La Sierrita	Fe-rich spherules	Avg.		24.82		25.37	10.49	0.16	0.36	0.09		0.04	20.37	87.1
Schulte et al., 2006		SD		1.44		0.79	0.41	0.13	0.09	0.08		0.04	0.86	
La Sierrita	Fe-rich spherules	Avg.		25.45		25.45	26.27	11.28	0.09	0.43		0.02	20.96	84.86
Schulte et al., 2006		SD		2.25		2.25	1.09	0.54	0.09	0.23		0.01	1.42	
La Sierrita	K-rich spherules	Avg.		1.88		50.23	2.35	7.25	0.57	0.19		0.1	29.15	91.79
Schulte et al., 2006		SD		0.54		1.16	0.29	0.21	0.07	0.13		0.04	0.78	
La Sierrita	K-rich spherules	Avg.		1.49		50.12	2.14	7.14	0.56	0.15		0.1	29.55	91.3
Schulte et al., 2006		SD		0.09		0.62	0.07	0.19	0.05	0.1		0.04	0.46	

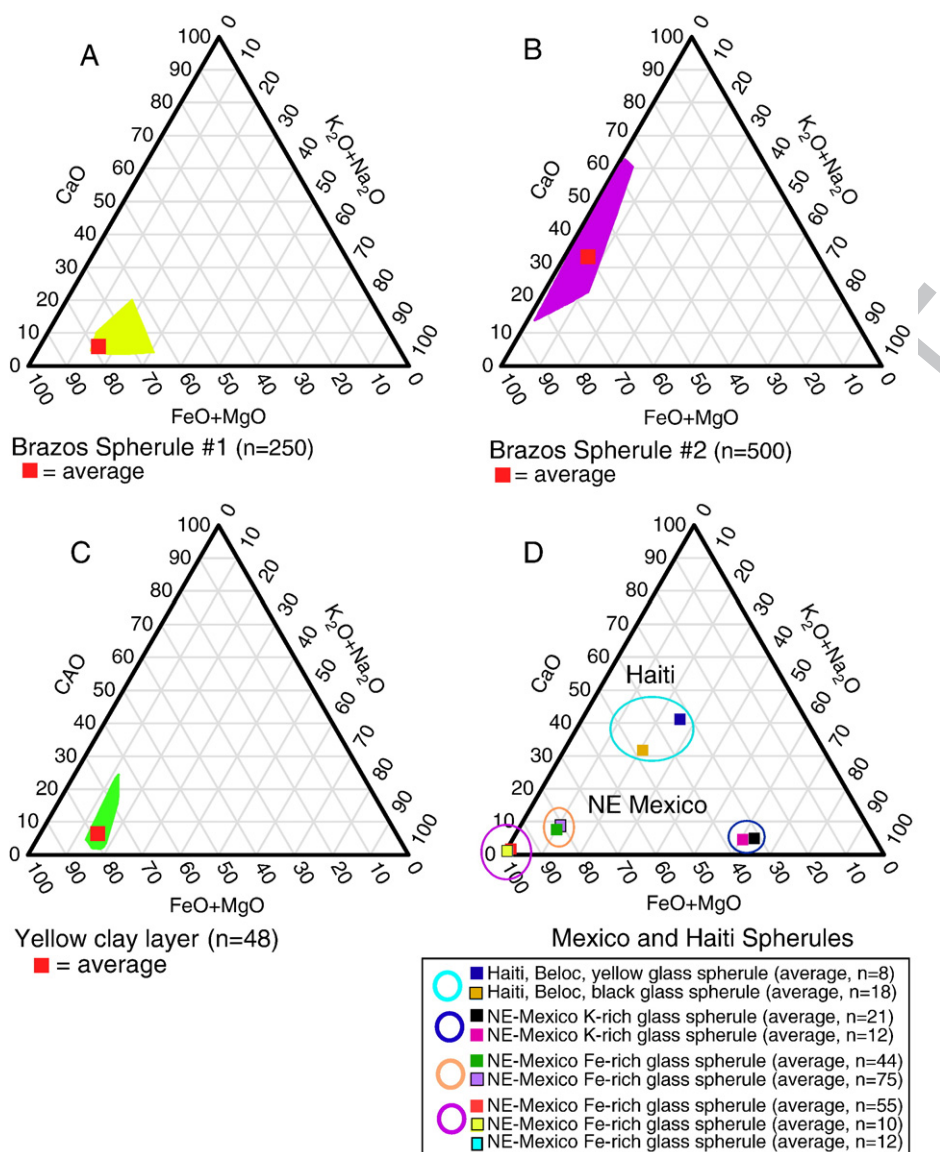
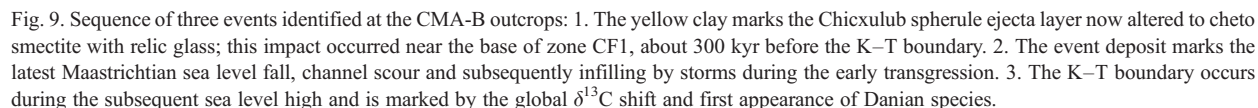
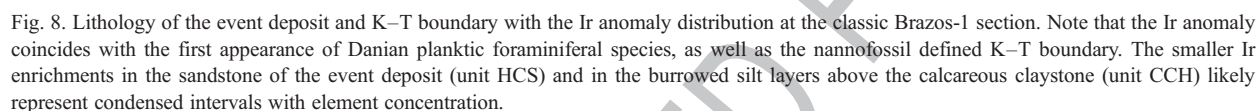


Fig. 7. Ternary plots ( $\text{K}_2\text{O}+\text{Na}_2\text{O}$ ,  $\text{FeO}+\text{MgO}$  and  $\text{CaO}$ ) show Brazos spherule samples from the event deposit unit BCB (A), unit SCS (B) and smectite altered spherules from the yellow clay (C) compared with spherules from NE Mexico and Haiti (D) [13,23–25]. Note that the yellow clay layer and Brazos spherule #1 samples have very similar compositions, which correlate well with Fe-rich glass spherules from NE Mexico. The lower FeO and higher CaO of Brazos spherule #2 sample reflects increased weathering.

517 cristallinity index,  $0.5$  to  $0.8^\circ 2\theta$  [19,20], with the 060  
518 reflection around  $61^\circ$  indicating a composition  
519 corresponding to nontronite, or cheto Mg-smectite. In  
520 contrast, smectite in Maastrichtian and Danian clays-  
521 tones is a common montmorillonite derived from  
522 weathering of soils, as indicated by the 060 reflection  
523 between  $61.7^\circ$  and  $62.3^\circ$  [26]. This coincidence in  
524 mineral composition strongly suggests a common origin  
525 for the yellow clay and the spherule-rich layers in unit

SCS of the event deposit, which are identified as  
Chicxulub impact spherules (Fig. 5). Geochemical  
analyses of the smectite phases from the yellow clay  
layer and from the spherule-rich sandstone layers  
support this conclusion (Table 1). All three layers are  
similar and reveal typical Mg enriched cheto type-  
smectite high in  $\text{SiO}_2$  (66–71%),  $\text{Al}_2\text{O}_3$  (19–20%), FeO  
(4.4–4.8%), MgO (2.8–3.3%) with minor  $\text{K}_2\text{O}$  (1–  
1.1%) and NaO (<0.5%). This composition is very





similar to the altered smectite rims from Haiti glass spherules and to NE Mexico glass spherules (Fig. 7A and B, Table 1).

## 5. Discussion

### 5.1. Placement of K–T boundary at Brazos

There is considerable disagreement in the placement of the K–T boundary in the Brazos sections because the paleontologically defined K–T occurs significantly above the event deposit. One group justifies the base of the event deposit as the K–T boundary based on the interpretation that it was generated by the Chicxulub impact, which is assumed to be of K–T age. Evidence cited in support of this interpretation includes the presence of impact spherules near the base and small Ir concentrations within the laminated sandstone layers near the top of the HCS unit and immediately above the calcareous claystone unit (Fig. 8). Yancey [9] termed this the event deposit defined K–T boundary. In this scenario, the interval between the event deposit and the paleontologically defined K–T boundary is interpreted as settling from the water column after the tsunami [2,3,7,10–12]. The K–T defining criteria do not support this boundary placement.

The other group (mostly paleontologists) uses the internationally accepted paleontologic, oceanographic and geochemical criteria to define and identify the K–T boundary horizon, including the mass extinction of all large tropical–subtropical planktic foraminiferal species, the first appearance of Danian species (in planktic foraminifera, palynomorphs), the Ir anomaly and  $\delta^{13}\text{C}$  shift. All of these markers, except the sudden mass extinction in planktic foraminifera, are present in the Brazos sections in the stratigraphic interval above the event deposit that varies from 20–30 cm (Brazos-1 and CMA-B sections) to 80 cm (Mull-1 core) [9,13,27]. The sudden mass extinction of all tropical–subtropical planktic foraminifera is diminished in the Brazos region because this species group is extremely rare or absent in the very shallow, low oxygen depositional environment that prevailed at Brazos during the latest Maastrichtian. The Ir anomaly is complex (Section 5.2), but shows the major enrichment at the paleontologically defined K–T boundary [28–30].

A critical and excellent K–T defining criterion is the negative  $\delta^{13}\text{C}$  shift that marks the boundary event globally coincident with the mass extinction and first appearance of Danian species. At Brazos, the onset of this negative shift has been documented in various sections between 20 cm to 30 cm above the event

deposit in the Cottonmouth Creek KT3 core [13,30] and the nearby CMA-B outcrops (Fig. 3A), 80 cm above in core Mull-1 (Fig. 3B) and 1.6 m above in the old core KT1 drilled at the same location as Mull-1 [13, unpublished]. In each section the  $\delta^{13}\text{C}$  shift coincides with the first appearances of Danian planktic foraminifera and palynomorphs, though nannofossils at Mull-1 show the high stress biotic changes earlier, at 43 cm above the event deposit. This apparent diachroneity may be due to the very shallow marine environment of the Brazos area and requires further study. The double thickness in core KT1, compared with 80 cm in Mull-1 may be an artifact of the drilling disturbance that led to redrilling in core KT2 [Hansen pers. communication 1988, 2005]. Thus, based on global paleontologic and oceanographic proxies ( $\delta^{13}\text{C}$  shift), the K–T boundary occurs well above (30–80 cm) the top of the event deposit. The argument that the K–T boundary should be placed at the base of the event deposit due to the presence of Chicxulub spherules [2,3,11,12] is not supported by standard K–T identifying criteria, or by sedimentologic characteristics (e.g., truncated burrows, multiple upward fining sequences), or Chicxulub ejecta layers (e.g., clasts with spherules indicating original deposition in older sediments; discovery of original ejecta layer below event deposit).

### 5.2. Iridium anomaly

The Ir anomaly is a critical K–T marker and also considered strong evidence for a large impact, generally believed to be the Chicxulub crater. However, no anomalous concentrations of Ir have ever been observed associated with Chicxulub spherule ejecta – not in the reworked spherule layer at the base of the event deposit or in the original ejecta layer below – in the expanded sequences of Brazos, NE Mexico, Haiti, Guatemala or Belize [4,23]. This suggests that the Chicxulub impact was not Ir-enriched. The Ir profile known from the classic Brazos-1 section (Fig. 1) is instructive. Three different laboratories have detected the same pattern with the maximum enrichment (1.5 to 2 ppb) in a 3–4 mm thick brown clay layer and overlying a 1 cm rusty red sandstone [26–28], coincident with the nannofossil abundance changes that are used to identify the K–T boundary [27] (Fig. 8). However, in view of the possibly diachronous occurrence of the nannofossil abundance changes in the Brazos area, this assignment is currently under review (Thibault and Gardin, written communic. 2006). In the event deposit, two enrichments of 0.3 to 0.4 ppb and 0.4 to 0.5 ppb occur in the laminated and burrowed fine sand near the top of the HCS unit and just



above the calcareous claystone unit (CCH), respectively. Similar minor Ir enrichments were also observed in the CMA-B and Mull-1 sections in burrowed and condensed intervals, which generally concentrate elements [31]. But the K–T boundary anomaly has not been detected to date in the new sections, though further analysis is continuing.

### 5.3. Age of event deposit

In Mull-1 and CMA-B sections, low diversity microfossil assemblages present below the event deposit indicate the latest Maastrichtian nannofossil *Micula prinsii* and planktic foraminifer CF1 zones, as also observed in Brazos-1, cores KT2, KT3 and other outcrops (Fig. 1) [13,14,27]. The CF1 index species (*Plummerita hantkeninoides*), which spans the last 300 ky of the Maastrichtian [31] first occurs 60 cm below the base of the event deposit in the CMA-B section. Above the event deposit, similar late Maastrichtian assemblages are present, though less abundant due to the shallower low oxygen environment. This indicates that the event deposit is older than the K–T boundary, but significantly younger than the yellow clay Chicxulub ejecta layer 40 cm below in the CMA-B section (Fig. 9).

Absolute age for the event deposit is difficult to estimate because the interval eroded at the base is unknown. From field observations, Gale [10] estimated that channels cut down to a maximum 1–1.5 m. If we assume the maximum undisturbed sedimentation from the event deposit to the K–T at 80 cm (Mull-1) and from the base of CF1 to the event deposit at 60 cm (CMA-B), plus the maximum down cutting of the channel at 1.5 m, then zone CF1 spans about 3 m, or about 1 cm/ka. This sedimentation rate is comparable to shallow water sequences in Egypt, Israel and Tunisia and comparable to the 1.25 cm/ka estimated by Schulte et al. [13] for the combined zone CF1 and CF2 interval in core KT2. By this estimate, the event deposit predates the K–T boundary by at least 80 kyr and postdates the Chicxulub impact (yellow clay) by at least 200 kyr.

### 5.4. Origin of event deposit

Although a number of studies have interpreted the event deposit as the result of an impact-generated tsunami wave with heights of 50–100 m and deposition in a single day followed by weeks of settling [2,8,12,13], sedimentologic features are incompatible with this interpretation. For example, a tsunami is most unlikely to erode discrete parallel channels [9,10]. The

truncated burrows at several horizons within the event deposit [10, this study] indicate long periods of non-deposition effectively ruling out a single tsunami event, but suggesting multiple storm events. This is also indicated by the large clasts of the basal conglomerate [9], the well-sorted sand, and multiple episodes of suspension settling, the three upward fining and truncated spherule-rich units of SCS in Mull-1, the burrowed and truncated HCS and burrowed CCH units. Microfossil assemblages present in unit HCS have the same species abundances as below and above the event deposit, with no exotic species present, which suggest a nearby sediment source. Moreover, the discovery of clasts with Chicxulub impact spherules in the basal conglomerate (unit BCB) indicates erosion of a pre-existing spherule–ejecta layer and also effectively rules out the impact–tsunami interpretation. Event deposition was most likely associated with a series of storms during a low sea level near the end of the Maastrichtian [9,10].

During the Late Maastrichtian the Brazos environment shallowed from middle to inner neritic depths [32] where channels were scoured during a major sea level fall (sequence boundary, Fig. 9) [33,34]. Gale [10] noted that reworked, bored and encrusted phosphatized concretions suggest lengthy exposure prior to infilling of the channels. This is consistent with clasts that contain cracks infilled by sparry calcite and spherules prior to erosion (Fig. 4). A time of erosion and/or non-deposition is also suggested by the abrupt disappearance of several species at this horizon [14], sometimes erroneously interpreted as the K–T mass extinction [13]. During the early transgression, the channels began to infill, first with the basal conglomerate, followed by repeated upward fining coarse glauconite, phosphatized clasts, shells and impact spherules and ending with fine sandstone. With the continuing transgression upward fining sands were deposited (unit HCS), frequently burrowed and truncated prior to renewed influx presumably generated by storm events [9,10]. The calcareous claystone (unit CCH) at the top of the event deposit shows upward fining grain size and increasing TOC suggesting settling of fines from the water column and a gradual return to normal marine sedimentation (Fig. 9). Above this interval, the gradual transition from calcareous silts to mudstone and claystone with burrows infilled by framboidal pyrite indicates a low oxygen environment [21] and maximum flooding surface by K–T boundary time.

### 5.5. Age of Chicxulub impact

The discovery of Chicxulub impact spherules in clasts at the base of the event deposit provides very strong

evidence that the impact occurred earlier. These spherule-bearing clasts must have been derived from an older spherule-rich deposit, which lithified over time and was subsequently exposed to erosion and transported during the event that scoured the channel of the event deposit. Thus, the spherule-bearing clasts reveal the geologic history of the spherules after the Chicxulub impact. In this case, the critical information revealed by these clasts is that the Chicxulub impact occurred well before the scour and event deposition, and also predated the K–T event. The yellow clay with cheto smectite, which is indicative of altered impact glass, was discovered in the CMA-B section near the base of zone CF1 and reveals that the Chicxulub impact occurred about 300 kyr prior to the K–T boundary (Fig. 9). This discovery is in agreement with the findings of thick Chicxulub spherule layers near the base of zone CF1 at Loma Cerca and El Penon, where 4–9 m of normal late Maastrichtian marls separate these spherule layers from the overlying sandstone complex or event deposits [4]. It is also in agreement with the findings in the Chicxulub crater core Yaxcopoil-1 where 50 cm of pelagic micritic limestone with five thin glauconitic clay layers and burrows separate the impact breccia from the K–T boundary [6,7].

#### 5.6. Chicxulub and the K–T mass extinction

The 300,000 yr pre-K–T age of the Chicxulub impact that has been documented from sections in NE Mexico [4], the Chicxulub crater [6,7] and now also from the Brazos River area in Texas, reveals that this impact was not responsible for the K–T mass extinction. The global distribution of an Ir anomaly at the K–T boundary suggests that another impact, coincident with Deccan volcanism and climate change, may have caused the mass extinction. What biotic effects can be attributed to the pre-K–T Chicxulub impact? Preliminary quantitative data from the Brazos sections indicate that no species extinctions and no significant changes in species abundances can be attributed to this impact event among planktic foraminifera, palynomorphs or nannofossils. The long-term biotic stress observed during the late Maastrichtian began prior to the Chicxulub impact and can be attributed to the sea level fall from about 80 m to 30 m or less at the time of the event deposition. The shallowing environment gradually and selectively eliminated deeper dwelling species and favored the survival of surface dwellers and low oxygen tolerant species. It is likely that the Chicxulub impact exacerbated the already deteriorating environmental conditions in the Brazos area, but did not cause any species extinctions.

## 6. Conclusions

The new Brazos core Mullinax-1 and new outcrops from Cottonmouth Creek provide critical new evidence regarding the placement of the K–T boundary, the age and origin of the event deposit and the age of the Chicxulub impact.

1. The K–T boundary, as recognized globally based on the first appearance of Danian species, the  $\delta^{13}\text{C}$  shift and the Ir anomaly, occurs well above the event deposit in Brazos sections. Low oxygen marine conditions prevailed during the latest Maastrichtian, as indicated by burrows infilled with framboidal pyrite and abundance of low oxygen tolerant benthic and planktic foraminifera in the interval between the top of the event deposit and the K–T boundary.
2. The event deposit infills a scoured channel (or incised valley) with multiple upward fining spherule-rich coarse sandstones, followed by hummocky cross-bedded sandstone, laminated sandstones and a calcareous claystone at the top. All of these units are frequently burrowed and truncated by erosion. These features are diagnostic of repeated storm deposition, rather than an impact-generated tsunami.
3. The basal conglomerate of the event deposit contains lithified mudstone clasts with Chicxulub impact spherules. This indicates Chicxulub ejecta fallout occurred prior to lithification, exposure, erosion, transport and redeposition of the clasts at the base of the event deposit.
4. The original Chicxulub ejecta layer was discovered 40 cm below the event deposit in the CMA-B section in a 3 cm thick yellow cheto smectite layer, which represent altered Chicxulub impact glass,
5. Spherule geochemistry of Chicxulub spherules from the event deposit and smectite altered spherules from the yellow cheto smectite clay are very similar and show a close correlation with Fe-rich spherules from NE Mexico.
6. The age of the Chicxulub impact can be estimated at  $\sim 300$  kyr prior to the K–T boundary based on the stratigraphic position of the yellow cheto smectite clay near the base of zone CF1, which spans the last 300 kyr of the Maastrichtian. This age estimate is consistent with earlier findings from NE Mexico and the Chicxulub crater core Yaxcopoil-1.

## 7. Uncited reference

[35]



830 **Acknowledgements**

831 We gratefully acknowledge the drilling crew of  
 832 DOSECC and logging support from Schlumberger  
 833 during two drilling phases. We thank Andrew Kerr  
 834 and one anonymous reviewer for their helpful com-  
 835 ments, Silvia Gardin and Nicolas Thibault for nanno-  
 836 fossil data and discussions, and Tom Yancey for his  
 837 invaluable help in the initial preparation and description  
 838 of the cores. We are grateful to Mrs. and Mr. Mullinax  
 839 for permission to drill on their land, their enthusiasm for  
 840 geological discoveries and delightful hospitality. Drilling  
 841 was supported by National Science Foundation  
 842 (NSF) Grant No. EAR-0447171. The research material  
 843 is based upon work supported by NSF grant EAR-  
 844 0207407, DFG grant PR 288/3-1, and Swiss FN-200020  
 845 105261/1.

846 **References**

- 847 [1] A.R. Hildebrand, G.T. Penfield, D.A. Kring, M. Pilkington, Z.Z.  
 848 Camargo, S.B. Jacobsen, W.V. Boynton, Chicxulub crater: a  
 849 possible Cretaceous/Tertiary boundary impact crater on the  
 850 Yucatan peninsula, Mexico, *Geology* 19 (1991) 867–871.
- 851 [2] J. Smit, T.B. Roep, W. Alvarez, A. Montanari, P. Claeys, J.M.  
 852 Grajales-Nishimura, J. Bermudez, Coarse-grained clastic sand-  
 853 stone complex at the K–T boundary around the Gulf of Mexico:  
 854 deposition by tsunami waves induced by the Chicxulub Impact,  
 855 *Geol. Soc. Am. Spec. Pap.* 307 (1996) 151–182.
- 856 [3] J. Smit, The global stratigraphy of the Cretaceous–Tertiary  
 857 boundary impact ejecta, *Annu. Rev. Earth Planet. Sci.* 27 (1999)  
 858 75–113.
- 859 [4] G. Keller, W. Stinnesbeck, T. Adatte, D. Stüben, Multiple  
 860 impacts across the Cretaceous–Tertiary boundary, *Earth-Sci.*  
 861 *Rev.* 62 (2003) 327–363.
- 862 [5] T. Adatte, W. Stinnesbeck, G. Keller, Lithostratigraphic and  
 863 mineralogical correlations of near-K–T boundary clastic sediments  
 864 in northeastern Mexico: Implications for mega-tsunami or sea level  
 865 changes? *Geol. Soc. Am. Spec. Pap.* 307 (1996) 197–210.
- 866 [6] G. Keller, T. Adatte, W. Stinnesbeck, M. Rebolledo-Vieyra, J.  
 867 Urrutia Fucugauchi, U. Kramar, D. Stueben, Chicxulub crater  
 868 predates K–T mass extinction, *Proc. Natl. Acad. Sci. U.S.A.* 101  
 869 (2004) 3753–3758.
- 870 [7] G. Keller, T. Adatte, W. Stinnesbeck, D. Stüben, Z. Berner, M.  
 871 Harting, More evidence that the Chicxulub impact predates the K–  
 872 T mass extinction, *Meteorit. Planet. Sci.* 39 (2004) 1127–1144.
- 873 [8] J. Bourgeois, T.A. Hansen, P. Wiberg, E.G. Kauffman, A tsunami  
 874 deposit at the Cretaceous–Tertiary boundary in Texas, *Science*  
 875 141 (1988) 567–570.
- 876 [9] T.E. Yancey, Stratigraphy and depositional environments of the  
 877 Cretaceous/Tertiary boundary complex and basal section, Brazos  
 878 River, Texas, Gulf Coast Assoc. Geol. Soc. Trans. 46 (1996)  
 879 433–442.
- 880 [10] A. Gale, The Cretaceous–Tertiary boundary on the Brazos River,  
 881 Falls County, Texas; evidence for impact-induced tsunami  
 882 sedimentation? *Proc. Geol. Assoc.* 117 (2006) 1–13.
- 883 [11] T.A. Hansen, R.B. Farrand, H.A. Montgomery, H.G. Billman,  
 884 G.L. Blechschmidt, Sedimentology and extinction patterns  
 across the Cretaceous–Tertiary boundary interval in east  
 Texas, *Cretac. Res.* 8 (1987) 229–252.
- 885 [12] D. Heymann, T.E. Yancey, W.S. Wolbach, H.M. Thiemens, E.A.  
 886 Johnson, D. Roach, S. Moecker, Geochemical markers of the  
 887 Cretaceous–Tertiary boundary event at Brazos River, Texas,  
 888 USA, *Geochim. Cosmochim. Acta* 62 (1998) 173–181.
- 889 [13] P. Schulte, R.P. Speijer, H. Mai, A. Kontny, The Cretaceous–  
 890 Paleogene (K–P) boundary at Brazos, Texas: Sequence stratig-  
 891 raphy, depositional events and the Chicxulub impact, *Sediment.*  
 892 *Geol.* 184 (2006) 77–109.
- 893 [14] G. Keller, Extended K–T boundary extinctions and delayed  
 894 populational change in planktic Foraminiferal faunas from  
 895 Brazos River Texas, *Paleoceanography* 4 (1989) 287–332.
- 896 [15] G. Keller, L. Li, N. MacLeod, The Cretaceous–Tertiary boundary  
 897 stratotype section at El Kef, Tunisia: how catastrophic was the  
 898 mass extinction? *Palaeogeogr. Palaeoclimatol. Palaeoecol.* 119  
 899 (1995) 221–254.
- 900 [16] A.A.A. Tantawy, Maastrichtian calcareous nannofossil biostrat-  
 901 igraphy and paleoenvironment of the Mahajanga Basin,  
 902 Madagascar, 3rd Proc. Int. Conf. Geology of Africa, Assiut,  
 903 Egypt, vol. 1, 2003, pp. 845–862.
- 904 [17] B. Kübler, Cristallinité de l'illite, méthodes normalisées de  
 905 préparations, méthodes normalisées de mesures, Neuchâtel,  
 906 Suisse, Cahiers Institute Géologie, Série ADX, 1, 1987 13 pp.
- 907 [18] F. Behar, V. Beaumont, B. De Pentadeo, Rock-Eval technology:  
 908 Performances and developments. Oil and Gas Science and  
 909 Technology, *Rev. Inst. Fr. Pet. (IFP)* 56 (2001) 111–134.
- 910 [19] P. Debrabant, E.E. Fourcade, H. Chamley, R. Rocchia, E. Robin,  
 911 J.P. Bellier, S. Gardin, F. Thiebault, Les argiles de la transition  
 912 Cretace-Tertiaire au Guatemala, temoins d'un impact d'asteroide,  
 913 *Bull. Soc. Geol. Fr.* 170 (1999) 643–660.
- 914 [20] G. Keller, W. Stinnesbeck, T. Adatte, B. Holland, D. Stueben,  
 915 M. Harting, C. de Leon, J. de la Cruz, Spherule deposits in  
 916 Cretaceous/Tertiary boundary sediments in Belize and Gua-  
 917 temala, *Geol. Soc. London* 160 (2003) 783–795.
- 918 [21] P.B. Wignall, R. Newton, M.E. Brookfield, Pyrite framboid  
 919 evidence for oxygen-poor deposition during the Permian–  
 920 Triassic crisis in Kahsmir, *Palaeogeogr. Palaeoclimatol. Palaeoecol.*  
 921 216 (2005) 183–188.
- 922 [22] M.L. Droser, D.J. Bottjer, A semiquantitative field classification  
 923 of ichnofabric, *J. Sediment. Res.* 56 (4) (1986) 558–559.
- 924 [23] D. Stüben, U. Kramar, M. Harting, W. Stinnesbeck, G. Keller,  
 925 T. Adatte, High resolution geochemical analysis of Creta-  
 926 ceous–Tertiary boundary sections in Mexico, *Geochim.*  
 927 *Cosmochim. Acta* 68 (2005) 1145–1172.
- 928 [24] P. Schulte, W. Stinnesbeck, D. Stueben, U. Kramar, Z. Berner,  
 929 G. Keller, T. Adatte, Fe-rich and K-rich mafic spherules from  
 930 slumped and channelized Chicxulub ejecta deposits in the  
 931 northern La Sierrita area, NE Mexico, *Int. J. Earth Sci.* 92  
 932 (2003) 114–142.
- 933 [25] G. Izett, Tektites in Cretaceous–Tertiary boundary rocks in  
 934 Haiti and their bearing on the Alvarez impact extinction  
 935 hypothesis, *J. Geophys. Res.* 96 (1990) 20879–20905.
- 936 [26] D.M. Moore, R.C. Reynolds, X-Ray diffraction and the  
 937 identification and Analyses of Clay Minerals, Oxford University  
 938 Press, Oxford, (1997) 378 pp.
- 939 [27] M.J. Jiang, S. Gartner, Calcareous nannofossil succession across  
 940 the Cretaceous–Tertiary boundary in east-central Texas, *Micro-  
 941 paleontology* 32 (1986) 232–255.
- 942 [28] R. Rocchia, E. Robin, L. Froget, J. Gayraud, Stratigraphic  
 943 distribution of extraterrestrial markers at the Cretaceous–Tertiary  
 944 boundary in the Gulf of Mexico area: implications for the  
 945

- temporal complexity of the event, *Geol. Soc. Am. Spec. Pap.* 307 (1996) 279–286.
- [29] H. Asaro, H.V. Michel, W. Alvarez, L.W. Alvarez, R.F. Maddocks, T. Burch, Iridium and other geochemical profiles near the Cretaceous–Tertiary boundary in a Brazos River section in Texas, in: R. Maddocks (Ed.), *Texas Ostracoda, Eight Int. Symp. on Ostracoda*, Houston, Texas, 1982, pp. 238–241.
- [30] R. Ganapathy, S. Gartner, M.J. Jiang, Iridium anomaly at the Cretaceous–Tertiary boundary in Texas, *Earth Planet. Sci. Lett.* 54 (1981) 393–396.
- [31] Z. Sawlowicz, Iridium and other platinum-group elements as geochemical markers in sedimentary environments, *Palaeogeogr. Palaeoclimatol. Palaeoecol.* 104 (1993) 253–270.
- [32] S.J. Culver, Benthic foraminifera across the Cretaceous–Tertiary (K–T) boundary: a review, *Mar. Micropaleontol.* 47 (2003) 177–226.
- [33] A.D. Donovan, R.G. Baum, G.L. Blechschmidt, T.S. Loutit, C.E. Pflum, P.R. Vail, Sequence stratigraphic setting of Cretaceous–Tertiary boundary in central Alabama, in: C.K. Wilgus, B.S. Hastings, C.G. Kendall, H.W. Posamentier, C.A. Ross, J.C. von Wagoner, (Eds.), *Sea Level Changes—an Integrated Approach*, SEPM Special Publication 42, pp. 299–307.
- [34] L. Li, G. Keller, T. Adatte, W. Stinnesbeck, Late Cretaceous sea level changes in Tunisia: a multi-disciplinary approach, *J. Geol. Soc. (London)* 157 (2000) 447–458.
- [35] E. Barrera, G. Keller, Stable isotope evidence for gradual environmental changes and species survivorship across the Cretaceous/Tertiary boundary, *Paleoceanography* 5 (1990) 867–889.